# Synthesis and Characterization of CaO-$SiO_2$ Heterogeneous Catalyst of Blood Cockle Shells and Coconut Fiber Ash for Biodiesel Production from Crude Palm Oil

**Nurhayati Nurhayati*, Muhdarina Muhdarina, Amilia Linggawati, and Siti Saidah Siregar**

*Department of Chemistry, Faculty of Mathematics and Natural Sciences, University of Riau, Kampus Bina Widya Km. 12.5, Simpang Baru, Pekanbaru 28293, Indonesia*

* ***Corresponding author:***

*email: nurhayati@lecturer.unri.ac.id*

*Received: December 5, 2023*
*Accepted: April 9, 2025*

**DOI:** 10.22146/ijc.91444

***Abstract:*** *The utilization of sustainable and renewable materials, specifically CaO derived from blood clam shells and $SiO_2$ extracted from coconut fiber, as catalysts for biodiesel production not only promotes waste valorization but also enhances catalytic efficiency, providing an eco-friendly and effective solution for biodiesel synthesis. The present study was synthesized and characterized CaO-$SiO_2$ catalysts using the impregnation method with $SiO_2$ content at 3, 5, and 7 wt.%. Characterization included surface area (BET), crystallinity and crystal size (XRD), chemical composition (XRF), functional groups (FTIR), and acidity-basicity (pyridine adsorption and titration). The maximum biodiesel yield of 96.29% was achieved under optimized conditions: 2 wt.% catalyst loading, 90-min reaction time, 60 °C temperature, and a 1:9 oil-to-methanol molar ratio, determined using response surface methodology (RSM). The synthesized biodiesel was evaluated according to ASTM D6751 standards, and its purity and methyl ester composition were analyzed using GC-MS. The results showed that the CaO-$SiO_2$ catalyst achieved a biodiesel purity of 97.44%, higher than that obtained with unmodified CaO. This research successfully modified the CaO-$SiO_2$ heterogeneous catalyst, enhancing its surface area and acidity, which led to an increase in the purity and yield of biodiesel synthesized from crude palm oil with high free fatty acid content.*

***Keywords:*** *biodiesel; blood cockle shell; CaO-$SiO_2$; coconut fiber ash; crude palm oil*

## ■ INTRODUCTION

The main energy source comes from fossil fuels which contribute 90% of the world's energy needs. It is projected that fossil fuel reserves could be depleted by 2050 [1]. With increasing awareness of environmental protection and decreasing annual petroleum reserves, biodiesel is becoming a focus as an environmentally friendly renewable alternative fuel. Of the various vegetable oils that have been used, crude palm oil (CPO) has significant potential as a sustainable feedstock for biodiesel production due to its abundance and good chemical composition. The problem with using CPO for biodiesel synthesis is the high free fatty acid (FFA) content (2–5%) [2-4], so if one uses a base catalyst, it will reduce the biodiesel yield due to the formation of soap or emulsion. Alternatives to increase the yield and characteristics of biodiesel, especially biodiesel made from raw materials that containing high FFA is to improve catalyst performance, including by increasing the surface area [5].

Previous studies have synthesized biodiesel from CPO using calcium oxide (CaO) as a heterogeneous catalyst [2]. CaO is an effective base catalyst with low solubility in methanol, simplifying its separation from the reaction mixture and enhancing reusability. Sources of CaO can be obtained from natural materials such as egg shells, crab shells, snail shells, and cockle shells [6]. Blood cockle shells has the potential as a heterogeneous catalyst because they contain calcium carbonate ($CaCO_3$) when calcined at 800 °C for 10 h, produced CaO more than 99% [7]. Cockle shells are rich in calcium content, primarily in the form of $CaCO_3$, which can be converted into CaO through calcination. Studies reveal that cockle shells are composed of approximately 98–99% $CaCO_3$, making them a highly valuable resource

for various applications. Their high calcium content allows for effective conversion into CaO through calcination, which is extensively utilized as a heterogeneous catalyst in biodiesel synthesis and serves as a key material in numerous industrial processes [8].

Biodiesel synthesis using the heterogeneous CaO catalyst has been widely carried out. Nurhayati et al. [7] synthesized a CaO catalyst from blood clam shells calcined at 800 and 900 °C for 10 h and used it for production of biodiesel based on used cooking oil. The maximum biodiesel yield obtained was 82.25% achieved at 60 °C, and a reaction time of 3 h. Despite the relatively high biodiesel yield, there is still opportunity for enhancement in catalytic activity to further enhance production efficiency. Efforts to increase biodiesel yields have included modifications to CaO catalysts through the incorporation of acids or bases. These modifications have been applied in both two-stage processes (involving esterification followed by transesterification) and one-stage processes (focused solely on transesterification) [2,9]. Such modifications aim to optimize catalyst performance, ensuring higher yields and improved reaction efficiency [4,10-13].

Two reaction stages, esterification and transesterification reactions, were performed to synthesize biodiesel using $H_2SO_4$ 3 M and CaO catalysts, respectively [2]. In this study, waste cooking oil (WCO) was used as a raw material, yielding 87.17% biodiesel under optimal conditions. The esterification process was optimized at 65 °C, a reaction time of 3 h, and an oil-to-methanol molar ratio of 1:24. In the transesterification stage, the highest yield was achieved using 3 wt.% CaO catalyst, a reaction temperature of 60 °C, a reaction time of 3 h, and an oil-to-methanol molar ratio of 1:6. Alias et al. [11] synthesized biodiesel by transesterification of WCO using CaO catalyst from limes stone with and without pretreated FFA. It showed that WCO with pretreated FFA using $H_2SO_4$ gave high methyl ester content compared to untreated FFA. Although the biodiesel yield through two reaction stages (esterification and transesterification) was quite high, this process increases the cost and operating time for making biodiesel. Several studies have also been carried out to develop methods by modifying CaO catalysts through impregnation supported by acid base or transition metal catalysts [4,9-15]. Modification of the CaO catalyst using $H_2SO_4$ was carried out by Nurhayati et al. [4]. The biodiesel yield obtained was quite high, namely 96.69%. However, using such an acid catalyst is not environmentally friendly if the remaining catalyst washing water is discharged into the environment. Nurhayati et al. [15] synthesized CaO from blood cockle shells modified with NaOH which was used in biodiesel synthesis and a 3% CaO/NaOH catalyst calcined at 873 K for 3 h producing a biodiesel yield of 89.25%.

Some researchers have also used porous materials, such as silica ($SiO_2$), to increase the surface area of CaO. $SiO_2$ is a porous solid with unique properties not found in other inorganic compounds, including chemical inertness, excellent adsorption capability, and ease of modification with specific chemicals to enhance its performance. Combining CaO with $SiO_2$ significantly increases the catalyst's surface area. Moreover, CaO is known to be less stable on its own, as it can readily react with atmospheric $CO_2$ and moisture, forming less active species like calcium hydroxide or $CaCO_3$. By combining CaO with $SiO_2$, the catalyst becomes more resistant to deactivation. Modification of the CaO-$SiO_2$ catalyst was carried out by Lani et al. [16] using CaO from cockle shells combined with $SiO_2$ from rice husk ash (5–50 wt.%). It showed an increase in the surface area of the CaO catalyst from 1.36 to 9.47 $m^2 g^{-1}$ after combining with $SiO_2$ (20 wt.%) and an increase in biodiesel yield to 85% attained at 6 wt.% catalyst dosage, 15:1 M ratio of methanol to oil, reaction temperature of 60 °C and reaction time of 2 h. When using 3 wt.% $SiO_2$ to CaO catalyst, the total surface area increased to 12.29 $m^2 g^{-1}$, and biodiesel yield became 87.5% at a reaction time of 2 h [17]. CaO-$SiO_2$ catalysts offer an efficient, cost-effective, and environmentally sustainable option for biodiesel production. The combination of CaO and $SiO_2$ creates a bifunctional catalyst system where CaO actively catalyzes the transesterification reactions, while $SiO_2$ catalyzes esterification ensures optimal distribution and stability of the active sites. This synergy effectively handles the challenges posed by high FFA content in

CPO, resulting in higher biodiesel yields and fewer side products.

Coconut husk is a waste that has significant potential as a raw material for $SiO_2$ production. The $SiO_2$ content in coconut husk increases by up to 90% after chemical treatment using acids or bases such as $H_2SO_4$ and NaOH [18-19]. In this research, the synthesis of the CaO-$SiO_2$ heterogeneous catalyst was carried out, where CaO was derived by calcining clam shells 5 h at 900 °C, while $SiO_2$ was obtained through the extraction of coconut husk waste. The CaO-$SiO_2$ 3, 5 and 7 wt.% catalyst was characterized and used for biodiesel production from CPO. with condition optimization using response surface methodology (RSM) through experimental design in the form of Box-Behnken design (BBD). RSM is a set of mathematical and statistical tools for assessing problems in which numerous independent variables on a response, with the primary aim of optimizing this response. Optimizing these variables with RSM enhances both the efficiency and cost-effectiveness of biodiesel production, supporting a more sustainable overall process [20-21]. The main variables affecting biodiesel production optimization include catalyst weight, reaction time and reaction temperature. Adjusting these variables is essential to maximize yield, improve fuel quality, and enhance cost-efficiency in biodiesel production. The utilization of sustainable and renewable materials, specifically CaO derived from blood clam shells and $SiO_2$ extracted from coconut fiber, as catalysts for biodiesel production not only promotes waste valorization but also enhances catalytic efficiency, providing an eco-friendly and effective solution for biodiesel synthesis.

## ■ EXPERIMENTAL SECTION

### Materials

The materials used in this research were CPO which was taken at PT. Kuala Lumpur Kepong Berhad Dumai City, blood cockle shell (*Anadara granosa*), coconut husk (*Cocos nucifera*), methanol ($CH_3OH$, Merck), ethanol ($C_2H_5OH$, Merck), isopropyl alcohol ($C_3H_8O$, Merck), phenolphthalein indicator ($C_{20}H_{14}O_4$, Merck), hydrochloric acid (HCl, Smart Lab), potassium hydroxide (KOH, Merck), acetone ($C_3H_6O$, Merck), oxalic acid ($C_2H_2O_4$, Merck), benzoic acid ($C_7H_6O_2$, Merck), table vinegar ($CH_3COOH$ 2%), pyridine ($C_5H_5N$), Whatman 42 filter paper, filter paper, demineralized aqua (aqua DM), and distilled water.

### Instrumentation

Instrumentation used for characterization of the catalyst and biodiesel was an X-ray diffractometer (XRD) Bruker D8 Advance, equipped with Cu-Kα radiation for analyzed the type of mineral, crystal size, and crystallinity of the catalyst. X-ray fluorescence (XRF) for analyzed elemental compositions. Fourier transform infrared spectroscopy (FTIR) type IRprestige-21 from Shimadzu was used to analyze the functional groups and acidity of the catalyst within the wavenumber range of 4000–500 $cm^{-1}$. The Quantachrome surface area analyzer (SAA) model a St 2 on NOVA touch 4LX was employed to assess the surface area and pore distribution through $N_2$ adsorption at 77 K using the Brunauer-Emmett-Teller (BET) technique. Meanwhile, gas chromatography-mass spectrometry (GC-MS) Agilent was utilized to determine the purity and chemical composition of the biodiesel yield.

### Procedure

#### *Synthesis of CaO catalyst*

Blood clam shell waste (BCS) was obtained from a seafood restaurant in the city of Pekanbaru. BCS was first cleaned and soaked in a vinegar solution overnight to remove impurities attached to the shell. BCS was rinsed and dried in an oven for ±24 h. The dried BCS was crushed and sieved through a 200-mesh and stored in a desiccator. BCS powder was calcined at 900 °C for 5 h to decompose $CaCO_3$ into CaO [4,7].

#### *Preparation of $SiO_2$*

The coconut husk was cut into small pieces, washed with distilled water and dried in the sun, then burned at 700 °C for 2 h. An amount of 10 g of coconut husk ash was dissolved in 40 mL of 3 M HCl, then stirred using a magnetic stirrer with a stirring speed of 600 rpm for 1 h at room temperature [16]. The mixture was filtered using Whatman 42 filter paper and washed with

hot aqua DM (80 °C) until the pH of the filtrate was neutral. The residue obtained was dried in an oven at 105 °C for ±24 h and calcined at 700 °C for 2 h.

### *Synthesis of CaO-$SiO_2$ catalyst*

The synthesis of CaO-$SiO_2$ catalyst was carried out using a wet impregnation method [16]. An amount of 10 g of CaO was suspended in 100 mL of aqua DM. The CaO suspension was added into a three-neck flask containing $SiO_2$ powder (variations 3, 5 and 7 wt.%). The mixture was refluxed with a stirring speed of 150 rpm at 80 °C for 4 h. The mixture was dried in the oven for ±24 h and calcined at 700 °C for 3 h.

### *Biodiesel synthesis*

Biodiesel was synthesized via transesterification reaction in a 500 mL three-neck round flask. A mixture of catalyst (variations 1, 2, and 3%) and methanol (1:9 ratio of oil to methanol) was refluxed for ±1 h. The mixture of catalyst and methanol was then filtered using Whatman 42 filter paper to separate the catalyst. CPO at 50 °C was added to the filtered methanol, then refluxed with a stirring speed 500 rpm for 90 min. After the reaction was complete, the mixture was put into a separating funnel and left overnight. The resulting biodiesel was washed using aqua DM and filtered using Whatman 42 filter paper to obtain crude biodiesel [15]. Repetition was carried out for all optimization variations of catalyst weight (1, 2 and 3 wt.%), reaction time (60, 90 and 120 min) and reaction temperature (55, 60 and 65 °C) according to optimization data using the BBD optimization from the RSM. The same treatment was carried out using a CaO-$SiO_2$ 3, 5 and 7 wt.% catalysts. To examine the effect of $SiO_2$ content on biodiesel yield, experiments were conducted under optimum conditions determined through RSM experimental design. CaO-$SiO_2$ catalysts with 3, 5, and 7 wt.% $SiO_2$ content was used, following the same procedure as in previous biodiesel synthesis.

## ■ RESULTS AND DISCUSSION

### XRD Analysis

XRD analysis was carried out to determine the type of mineral of the CaO-$SiO_2$ catalysts (3, 5, and 7% $SiO_2$). The catalyst diffractogram results were compared with standard diffractograms or the Join Committee Powder Diffraction Structure (JCPDS) [22]. Based on the results of the diffractogram in Fig. 1, peaks are obtained which indicate the presence of the minerals lime (CaO) at 2θ = 32.23, 37.41, 53.92, 64.23 and 67.24°, portlandite ($Ca(OH)_2$) at 2θ = 17.96, 28.64, 34.19, 47.51, 50.80 and 79.67°. The appearance of the CaO peaks in the diffractogram indicates that the calcination process carried out at a temperature of 900 °C for 5 h has succeeded in decomposing the mineral calcite ($CaCO_3$) into CaO. The peak of portlandite ($Ca(OH)_2$), which is still often found is caused by CaO reacting with water vapor or being exposed to air in the catalyst synthesis since CaO is a hygroscopic compound [23-24]. In addition to CaO and $Ca(OH)_2$ peaks, a peak of $CaSiO_3$ also appears at 2θ = 34.19° that is a possibility of overlapping with $Ca(OH)_2$ peaks. This is in accordance with research by Lani et al. [16], which states that calcium silicate $CaSiO_3$ and $Ca_2SiO_4$ are found at 29.4 and 34.2°. The appearance of the $CaSiO_3$ peak proves that CaO has reacted with $SiO_2$ during the impregnation process. The coconut husk diffractogram shows the presence of a broad $SiO_2$ peak at 21.71°. The same result was found by Hadiyanto et al. [25]. $SiO_2$ found at 21°; however, the XRD diffractogram shows that it is in the amorphous phase. It is known that $SiO_2$ calcined at 700 °C still shows an amorphous structure [26]. Apart from that, the diffractogram of coconut coir $SiO_2$ also shows $K_2O$ and $P_2O_5$ peaks at 31 and 41° [18]. The inherent

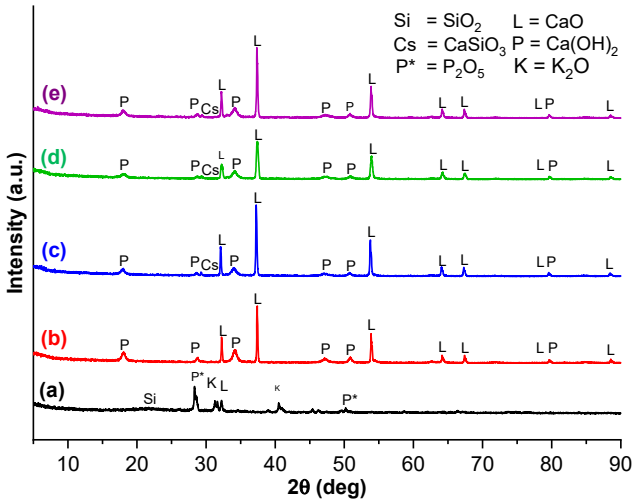


**Fig 1.** XRD pattern of (a) $SiO_2$, (b) CaO, (c) CaO-$SiO_2$ 3%, (d) CaO-$SiO_2$ 5%, and (e) CaO-$SiO_2$ 7%

mineral composition of coconut husk, particularly its potassium and phosphorus content, can result in the presence of $K_2O$ and $P_2O_5$ in the extracted $SiO_2$.

An increase in intensity is observed in the XRD diffractogram after modifying CaO with 3% $SiO_2$. The interaction between $SiO_2$ and CaO could lead to the formation of new crystalline phases, such as $CaSiO_3$, which typically exhibit distinct diffraction patterns with higher intensity compared to unmodified CaO. However, the XRD peak intensity of CaO-$SiO_2$ 5% is lower than 3 and 7% CaO-$SiO_2$. Increasing the $SiO_2$ content to 5% might introduce excess amorphous material into the system. This additional amorphous phase could disrupt the crystallinity of CaO or the newly formed phases, reducing diffraction intensity. Additionally, the increased $SiO_2$ content could influence crystallite size or induce partial amorphization, which can alter the XRD peak intensities. The average crystallite size and crystallinity of the $SiO_2$, CaO, and CaO-$SiO_2$ catalysts with 3, 5, and 7% $SiO_2$ content, as summarized in Table 1, were analyzed using Origin Pro Software. Crystallinity was calculated by comparing the crystalline area fraction with the total area fraction, which includes the crystalline and amorphous area fractions, while the crystallite size was calculated using the Debye-Scherrer equation [27].

According to the data presented in Table 1, the crystallite size and crystallinity of the CaO-$SiO_2$ catalyst decrease at 5% $SiO_2$ content but increase again at 7%. It can be explained by the interplay of factors affecting nucleation, crystal growth, and $SiO_2$ dispersion in the catalyst matrix. The presence of $SiO_2$ at specific levels can cause partial amorphization or create structural heterogeneity, as some $SiO_2$ remains poorly integrated, leading to reduced XRD peak intensity (as seen in Fig. 1) and lower crystallinity [28].

## XRF

The chemical composition of purified $SiO_2$ coconut husk was analyzed using XRF. The results obtained can be seen in Table 2. The data indicate that the CaO composition decreases as the $SiO_2$ composition increases from 3 to 7% in the CaO-$SiO_2$ catalysts. The 3% CaO-$SiO_2$ catalyst exhibits the highest CaO content at 96.981%. Conversely, the 5% CaO-$SiO_2$ catalyst shows the highest $SiO_2$ content, reaching 1.006%. The CaO-$SiO_2$ (5% $SiO_2$) catalyst exhibits the highest $SiO_2$ content compared to the 3 and 7% variations, likely due to the optimal integration of $SiO_2$ within the catalyst matrix at this specific percentage [29]. At lower $SiO_2$ levels (3%), the incorporation might be insufficient, while at higher

**Table 1.** Analysis result of the average crystallite size and crystallinity of the $SiO_2$, CaO, CaO-$SiO_2$ samples

| Catalyst | Average crystallite size (nm) | Crystallinity (%) |
|---|---|---|
| $SiO_2$ | 22.327 | 17.296 |
| CaO | 29.324 | 45.238 |
| CaO-$SiO_2$ 3% | 24.761 | 43.113 |
| CaO-$SiO_2$ 5% | 18.040 | 41.254 |
| CaO-$SiO_2$ 7% | 21.866 | 42.496 |

**Table 2.** Results of analysis of the chemical composition of $SiO_2$, CaO, CaO-$SiO_2$ catalysts using XRF

| Compound | Composition (%) | | | | |
|---|---|---|---|---|---|
| | $SiO_2$ | CaO | CaO-$SiO_2$ 3% | CaO-$SiO_2$ 5% | CaO-$SiO_2$ 7% |
| CaO | 23.124 | 98.142 | 96.981 | 96.309 | 96.418 |
| $SiO_2$ | 37.174 | - | 0.692 | 1.006 | 0.928 |
| $K_2O$ | 14.862 | - | - | - | - |
| $P_2O_5$ | 10.284 | 0.702 | 0.580 | 0.933 | 0.953 |
| $In_2O_3$ | - | - | 0.631 | 0.945 | 0.991 |
| $Ag_2O$ | 0.308 | 0.509 | 0.112 | 0.047 | 0.024 |
| $Al_2O_3$ | - | 0.301 | 0.350 | 0.343 | 0.234 |
| $Fe_2O_3$ | 0.614 | 0.013 | 0.022 | 0.026 | 0.030 |
| SrO | 0.057 | 0.293 | 0.219 | 0.205 | 0.173 |

levels (7%), challenges like agglomeration or uneven dispersion can occur, reducing effective surface exposure. Studies have shown that $SiO_2$ content and dispersion depend on preparation methods and ratios, impacting final catalyst properties [30].

Table 2 also reveals that the CaO-$SiO_2$ (3, 5, and 7% $SiO_2$) catalysts contain trace amounts of additional oxide compounds, including $P_2O_5$, $In_2O_3$, $Ag_2O$, $Al_2O_3$, $Fe_2O_3$, and SrO. The leaching process on coconut husk using HCl is known to increase the $SiO_2$ purity because other metal oxides are reduced due to dissolution in HCl [31]. Based on the results obtained, the percentage of $SiO_2$ produced is still very small. This is because there are still many impurity compounds that have not been completely reduced from the leaching process using HCl as evidenced by the presence of other oxide components in the XRF results.

## FTIR Analysis

The functional groups of the CaO-$SiO_2$ (3, 5 and 7%) catalysts, as well as $SiO_2$ and CaO were analyzed using FTIR analysis at wavenumber between 400 and 4700 $cm^{-1}$ and the results are shown in Fig. 2. FTIR spectrum shows a sharp absorption band at 3638–3642 $cm^{-1}$ which indicates the presence of O–H stretching vibrations from $Ca(OH)_2$ [15], This is due to CaO being hydrated by water vapor since it is hygroscopic so it easily binds water molecules from free air, while the O–H groups presented in the $SiO_2$ catalyst come from its bond with water vapor. The wavenumber 1405–1411 $cm^{-1}$ showed the presence of O–C–O asymmetric stretching vibrations of monodentate carbonate on the CaO surface. Apart from that, $CO_3^{2-}$ was also found at 864–873 $cm^{-1}$, which is the bending vibration of C–O. The appearance of the stretching vibration of the $CO_3^{2-}$ group, is believed to be due to the chemisorption of gaseous $CO_2$ from the atmosphere over the surface of the catalyst [17], forming surface-bound carbonate species that are insufficient in quantity or crystallinity to produce distinguishable XRD patterns. At 1056–1087 $cm^{-1}$ and 803 $cm^{-1}$, it shows the existence of asymmetric stretching vibrations of the siloxane (Si–O–Si) group, which is caused by the addition of $SiO_2$ to the CaO catalyst. The wavenumber 952–953 $cm^{-1}$ shows the presence of the Si–O–Ca group, which

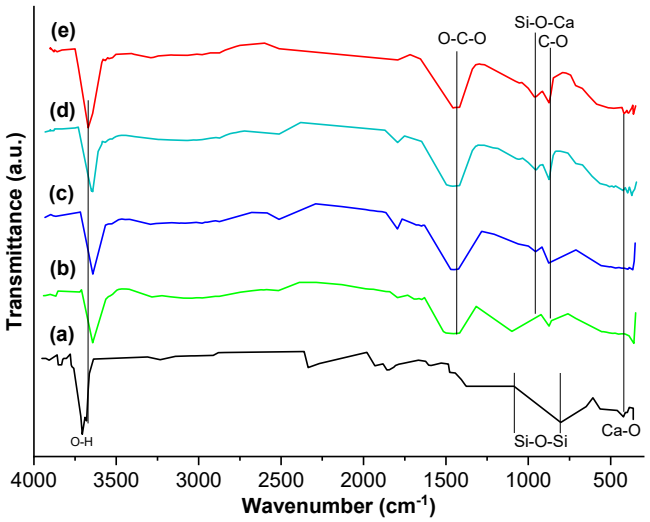


**Fig 2.** FTIR spectra of (a) $SiO_2$, (b) CaO, (c) CaO-$SiO_2$ 3%, (d) CaO-$SiO_2$ 5%, and (e) CaO-$SiO_2$ 7% catalysts

indicates that $SiO_2$ has been successfully impregnated with CaO. The interaction between CaO and $SiO_2$ under specific conditions, such as high temperature, can lead to the formation of new bonds, resulting in $CaSiO_3$ phases [17], which can also be confirmed through characterization techniques such as XRD (Fig. 1). The wavenumber 422–434 $cm^{-1}$ shows the presence of the Ca–O group, which indicates that the calcination process carried out at 900 °C for 5 h has succeeded in decomposing the mineral calcite ($CaCO_3$) into lime (CaO).

## BET Analysis

The surface area of the CaO-$SiO_2$ catalyst which has been synthesized using the impregnation method is determined using a surface area analyzer with the BET method. The surface area, pore volume and radius of the pores of the CaO-$SiO_2$ catalyst are shown in Table 3. The surface area of the CaO catalyst derived from waste cockle shell was determined as 1.227 $m^2\ g^{-1}$. Upon modification with $SiO_2$ of coconut husk, the surface area increased to a maximum of 7.109 $m^2\ g^{-1}$ in the CaO-$SiO_2$ (5%) catalyst. This increased due to a strong interaction between CaO and $SiO_2$, which slowing down diffusion of $Ca^{2+}$, restrained sintering and stabilized the CaO surface [15]. Therefore, CaO-$SiO_2$ catalyst is expected to achieve high catalytic activity and excellent stability compared to CaO catalyst. However, further increases in $SiO_2$ content (7%)

**Table 3.** The surface area of CaO, $SiO_2$, and CaO-$SiO_2$ catalysts

| Catalyst | Surface area ($m^2\ g^{-1}$) | Pore volume ($cm^3\ g^{-1}$) | Pore size (nm) |
|---|---|---|---|
| CaO | 1.227 | 0.003 | 2.760 |
| $SiO_2$ | 6.844 | 0.018 | 2.454 |
| CaO-$SiO_2$ 3% | 2.675 | 0.006 | 1.790 |
| CaO-$SiO_2$ 5% | 7.109 | 0.008 | 1.608 |
| CaO-$SiO_2$ 7% | 2.842 | 0.006 | 1.611 |

resulted in a decrease in surface area. The decrease in surface area of 3 and 7% $SiO_2$ is due to agglomeration on the catalyst surface. The agglomeration of $SiO_2$ particles as a gap between the particles will cause the Ca particles not to be dispersed optimally, resulting in lumps forming. At 5%, the $SiO_2$ content aligns with the CaO surface properties, ensuring uniform distribution and avoiding agglomeration.

## Acidity and Basicity Analysis

The acidity and basicity of a catalyst are crucial in biodiesel synthesis, as these characteristics directly influence the efficacy and selectivity of the transesterification reaction, the primary process in biodiesel production. The acidity of the catalyst was assessed by pyridine vapor adsorption and FTIR techniques [17], while its basicity was evaluated using acidimetric titration with phenolphthalein as an indicator. The analysis results of the acidity and basicity of the CaO-$SiO_2$ catalyst at 3, 5, and 7% concentrations are presented in Table 4. The results indicate that the CaO-$SiO_2$ 5% catalyst exhibits a higher acidity than the 3 and 7% CaO-$SiO_2$ catalysts, with a value of 0.2980 mmol $g^{-1}$. This indicates that the number of acid sites present in the catalyst depends upon the percentage of $SiO_2$ content. The proportion of $SiO_2$ in the catalyst is directly correlated with the number of acid sites present. This increase is attributed to the central acid core situated on the Si skeleton. Conversely, the acidity is inversely proportional to the CaO content, with higher CaO content in the catalyst resulting in lower acidity. This is supported by the data presented in Table 4, which indicates that the highest basicity is observed in catalysts with the lowest $SiO_2$ content. The presence of acidic and basic sites on the catalyst gives rise to a substitution reaction, or group replacement reaction, whereby acidic and basic groups from CaO and $SiO_2$ are replaced, resulting in a decrease in acidity with increasing catalyst basicity [32-33].

## RSM Optimization of Biodiesel Production

In this study, biodiesel synthesis was carried out using RSM experimental design method with Design Expert 12 software to obtain optimum conditions. The data used to create a model of the influence of variables were catalyst weight ($\xi_1$), reaction time ($\xi_2$) and reaction temperature ($\xi_3$) on the response (Y), namely biodiesel yield. Variables determined for operating conditions are entered into the BBD experimental design using variable codes in predetermined ranges. The research data was processed using statistics to determine its suitability for the model and the optimum biodiesel yield was found on the CaO-$SiO_2$ (5%) catalyst. The biodiesel yields synthesized using 5% CaO-$SiO_2$ catalysts are shown in Table 5.

Research results obtained from data in Table 5 processed according to RSM using statistics that produce ANOVA data on the experiments presented in Table 6. Based on Table 6, the F-value (92.79) exceeds the F-table value (4.77), leading to the rejection of $H_0$ and acceptance of $H_1$. This indicates that there is no lack of fit in the regression model. A high F-value and the absence of lack of fit confirm that the second-order regression model is well-suited for accurately explaining

**Table 4.** Acidity and basicity of the CaO-$SiO_2$ (3, 5 and 7%) catalyst

| Catalyst | Acidity (Amount of pyridine adsorbed; mmol $g^{-1}$) | Basicity (Amount of benzoic acid; mmol $g^{-1}$) |
|---|---|---|
| CaO | 0.239 | 1.800 |
| CaO-$SiO_2$ 3% | 0.274 | 1.633 |
| CaO-$SiO_2$ 5% | 0.298 | 1.533 |
| CaO-$SiO_2$ 7% | 0.286 | 1.333 |

**Table 5**. Biodiesel yield with $CaO\text{-}SiO_2$ (5%) catalyst

| No | Variable | | | Yield biodiesel (%) | Yield predicted (%) |
|---|---|---|---|---|---|
| | $\xi_1$ Catalyst concentration (wt.%) | $\xi_2$ Reaction time (min) | $\xi_3$ Reaction temperature (°C) | | |
| 1 | 1(-1) | 120(1) | 60(0) | 92.28 | 94.24 |
| 2 | 1(-1) | 90(0) | 65(1) | 88.56 | 89.19 |
| 3 | 1(-1) | 90(0) | 55(−1) | 94.05 | 94.13 |
| 4 | 1(-1) | 60(−1) | 60(0) | 92.75 | 93.04 |
| 5 | 2(0) | 120(1) | 65(1) | 86.81 | 88.56 |
| 6 | 2(0) | 120(1) | 55(−1) | 92.44 | 93.54 |
| 7 | 2(0) | 90(0) | 60(0) | 96.12 | 96.14 |
| 8 | 2(0) | 90(0) | 60(0) | 96.02 | 96.14 |
| **9** | **2(0)** | **90(0)** | **60(0)** | **96.29** | **96.14** |
| 10 | 2(0) | 60(−1) | 65(1) | 88.40 | 88.80 |
| 11 | 2(0) | 60(−1) | 55(−1) | 90.92 | 90.54 |
| 12 | 3(1) | 120(1) | 60(0) | 93.30 | 92.98 |
| 13 | 3(1) | 90(0) | 65(1) | 89.15 | 89.33 |
| 14 | 3(1) | 90(0) | 55(−1) | 91.64 | 91.11 |
| 15 | 3(1) | 60(−1) | 60(0) | 90.03 | 91.42 |

**Table 6.** ANOVA data quadratic model

| Source | Sum of squares | df | Mean square | F-value | p-value | F-table ($\alpha = 0.05$) |
|---|---|---|---|---|---|---|
| Model | 104.0100 | 9 | 11.5600 | 11.0600 | 0.0083 | |
| $X_1$-Catalyst weight | 4.1800 | 1 | 4.1800 | 4.0000 | 0.1020 | |
| $X_2$-Reaction time | 3.8900 | 1 | 3.8900 | 3.7300 | 0.1115 | |
| $X_3$-Reaction-temperature | 22.5100 | 1 | 22.5100 | 21.5500 | 0.0056 | |
| $X_1X_2$ | 0.0380 | 1 | 0.0380 | 0.0364 | 0.8562 | |
| $X_1X_3$ | 2.5400 | 1 | 2.5400 | 2.4300 | 0.1794 | 4.7700 |
| $X_2X_3$ | 2.6700 | 1 | 2.6700 | 2.5600 | 0.1706 | |
| $X_1^2$ | 6.3900 | 1 | 6.3900 | 6.1100 | 0.0563 | |
| $X_2^2$ | 13.3400 | 1 | 13.3400 | 12.7600 | 0.0160 | |
| $X_3^2$ | 55.6000 | 1 | 55.6000 | 53.2100 | 0.0008 | |
| Residual | 5.2200 | 5 | 1.0400 | - | - | |
| Lack of fit | 5.1900 | 3 | 1.7300 | 92.7900 | 0.0107 | |
| Pure error | 0.0373 | 2 | 0.0186 | - | - | |
| Total | 109.2300 | 14 | - | - | - | |

the observed data and effectively capturing the underlying relationships. The results of the data processing yield a second-order equation, as shown in Eq. (1):

$$y = 96.14 - 0.72X_1 + 0.69X_2 - 1.68X_3 + 0.09X_1X_2 + 0.79X_1X_3 - 0.81X_2X_3 - 1.32X_1^2 - 1.90X_2^2 - 3.88X_3^2 \quad (1)$$

The statistical model suggested by the design expert software is a quadratic model as presented in Table 7. Adjusted and predicted $R^2$ are statistical measures used in regression analysis to evaluate model performance. Adjusted $R^2$ is a modification of the standard $R^2$ that accounts for the number of predictors in the model. A high adjusted $R^2$ suggests a good fit. On the other hand, predicted $R^2$ evaluates the model's ability to predict new, unseen data. It measures the proportion of variation in the response variable that the model can predict. Based on Table 7, the $R^2$ value obtained from the regression model is 0.9522, which is close to 1. The adjusted R-square value is quite high, namely 0.8661, the highest

**Table 7.** Model summary statistics

| Variation | Std. Dev. | $R^2$ | Adjusted $R^2$ | Predicted $R^2$ | PRESS | |
|---|---|---|---|---|---|---|
| Linear | 2.67 | 0.2800 | 0.0836 | −0.1508 | 125.7000 | |
| 2FI | 3.03 | 0.3210 | −0.1759 | −0.9334 | 211.1900 | |
| **Quadratic** | **1.02** | **0.9522** | **0.8661** | **0.2395** | **83.0700** | **Suggested** |
| Cubic | 0.1365 | 0.9997 | 0.9976 | - | - | Aliased |

predicted R-square value is 0.2395, and the lowest PREES value is 83.07. A large difference between adjusted $R^2$ and predicted $R^2$ (> 0.2) indicates that the model may not predict new observations well, suggesting potential overfitting. This may be caused by too many predictors or overly complex interactions, which can cause the model to fit the noise in the data rather than the underlying trend, leading to poor predictive performance. However, the calculated F-value of the graphic equation obtained from the RSM results is 11.06, which indicates that the graphic equation is significant. So, it can be concluded that the results of statistical data processing are in accordance with the model [34].

## Effect of Process Conditions and Their Interactions on Biodiesel Yield

The results of the p-value test show that each variable has a significant influence on biodiesel yield, but the most influential is the reaction time. Fig. 3 shows that the catalyst interaction $X_1X_2$ represents the interaction between reaction temperature, time, and catalyst loading. The optimum conditions for biodiesel synthesis were achieved using a CaO-$SiO_2$ (5%) catalyst, with a reaction time of 90 min, a temperature of 60 °C, and a catalyst loading of 2 wt.%. At 60 °C, the reaction benefits from enhanced interaction between reactants and the catalyst, driven by more intense particle movement under these conditions. If the temperature exceeds 60 °C, the methanol will evaporate because it has reached the boiling point of methanol and the biodiesel yield will decrease. Using 2 wt.% of catalyst will cause an increase in biodiesel yield because methanol will react with the CaO catalyst to form $CH_3O^-$ ions so that the transesterification reaction takes place quickly. Still, if excess catalyst is used, it will form an emulsion due to saponification. It will cause agglomeration, which will reduce the solubility of methanol as well as oil so that the yield of biodiesel produced decreases. The more catalysts used in the synthesis process, the more soap will be produced, and the biodiesel yield will also decrease. The soap formed interferes with the separation process of glycerol and methyl ester. The formation of soap can also trap methyl esters in the glycerol phase, reducing the overall yield of biodiesel. This condition was obtained because the biodiesel yield increased from a reaction time of 60 to 90 min. This occurs when a reversible reaction occurs during the transesterification process. The reaction between the catalyst and FFA in CPO is the process of forming soap [35].

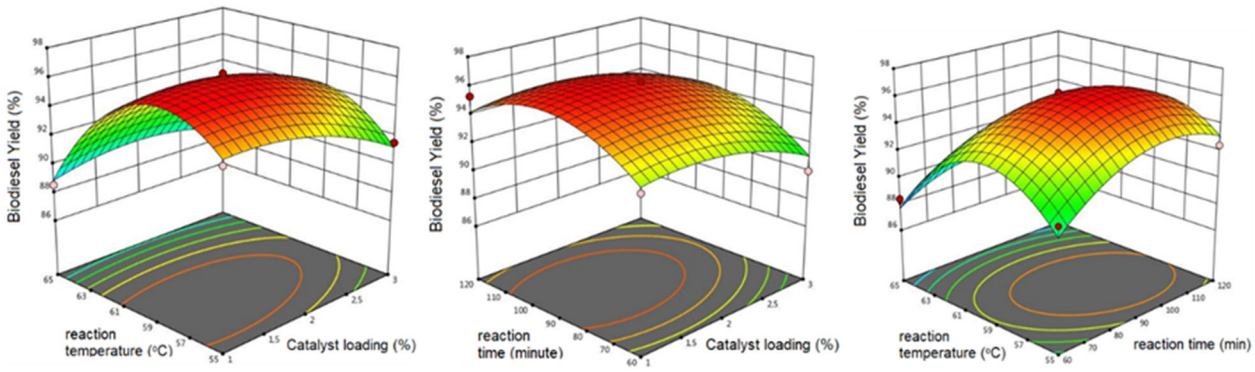


**Fig 3.** 3D surface plot showing the values of optimum biodiesel yield

### Effect of $SiO_2$ Content on Biodiesel Yield

The effect of $SiO_2$ content on the catalytic activity of CaO-$SiO_2$ catalysts (at 0, 3, 5, and 7% $SiO_2$) was evaluated under optimal conditions, including a reaction time of 90 min, a catalyst loading of 2 wt.%, a temperature of 60 °C, an oil-to-methanol molar ratio of 1:9, and stirring speed of 500 rpm. The impact of varying $SiO_2$ concentrations on biodiesel yield is presented in Fig. 4. The results indicate that the CaO-$SiO_2$ (5%) catalyst yields higher biodiesel production compared to both the CaO-$SiO_2$ (3 and 7%) catalysts. The higher biodiesel yield from 2.675 $m^2 g^{-1}$ on the CaO-$SiO_2$ (3%) catalyst to 7.109 $m^2 g^{-1}$ on the CaO-$SiO_2$ (5%) catalyst. The high surface area will increase the performance of the catalyst due to the strong interaction between CaO and $SiO_2$. This is supported by the FTIR results (Fig. 2) in which the wavenumber between 952–953 $cm^{-1}$ shows the presence of the Si–O–Ca group, which indicates that $SiO_2$ has been successfully impregnated with CaO. Moreover, higher $SiO_2$ content on the catalysts CaO will slow down the diffusion of $Ca^{2+}$, resist sintering and stabilize the CaO surface. Increasing the pore volume of the catalyst also causes sufficient space to allow reactant interactions to be more flexible [15]. However, the biodiesel yield using the CaO-$SiO_2$ (7%) catalyst decreased in line with the decreasing catalyst surface area, it is due to the covering of the active sites on the CaO surface by excess $SiO_2$, thereby reducing the catalytic activity (Fig. 4). Apart from the effect of a smaller surface area, the decrease in biodiesel yield is also caused by the presence of impurities or $H_2O$ from the air that are absorbed when weighing the catalyst before use for the transesterification process. In addition, using CaO-$SiO_2$ (5%) catalyst yields higher biodiesel production compared to the CaO-$SiO_2$ (7%) catalysts. Excessive amounts of $SiO_2$ in the CaO-$SiO_2$ catalyst can negatively affect biodiesel yield by causing agglomeration of catalyst particles. This agglomeration may hinder proper dispersion and reduce the number of active sites available for the transesterification reaction. Furthermore, higher catalyst loadings can increase the viscosity of the reaction mixture, leading to poor diffusion between the reactants and catalyst, which ultimately reduces methyl ester production [36].

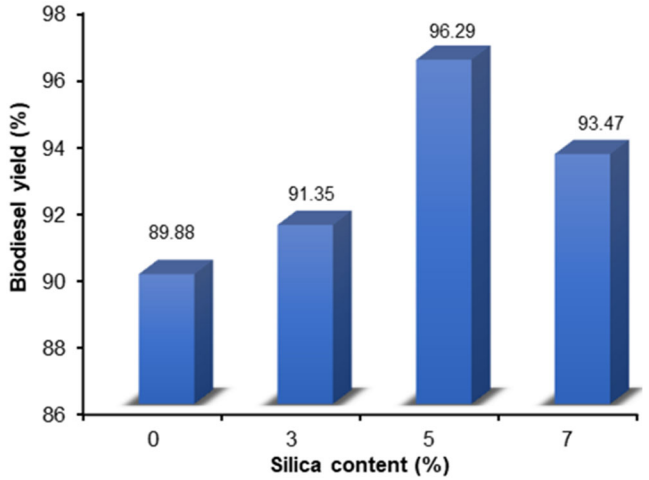


**Fig 4.** Effect of $SiO_2$ content on biodiesel yield

### Characteristics of Biodiesel

The optimum biodiesel produced in this study was characterized to assess its quality, which is crucial for ensuring effective and durable engine performance. Key parameters tested included methyl ester content, moisture content, specific gravity, viscosity, residual carbon, and acid number. The methyl ester content in the produced biodiesel was identified using gas chromatography-mass spectroscopy (GC-MS), and the results are presented in Fig. 5 and Table 8. The GC-MS analysis revealed that the major components of the biodiesel are methyl esters (97.44%), primarily methyl palmitate and methyl oleate.

The GC-MS results show that the biodiesel contains FAMEs ranging from C13 to C25, with C16–C19 being the most dominant, which is ideal for biodiesel applications. The biodiesel sample contains a mix of saturated and unsaturated FAMEs. The high content of saturated fatty acids, such as methyl palmitate (35.45%) and methyl stearate (7.95%), enhances the oxidation stability of biodiesel, as the single bonds in its carbon chain are more resistant to oxidation. The presence of unsaturated fatty acids, especially methyl oleate (45.53%), provides a balance between oxidation stability and low-temperature flow properties. Monounsaturated fatty acids tend to provide better oxidation stability than polyunsaturated fatty acids, while still maintaining good flow properties at low temperatures. Thus, the FAME composition in biodiesel

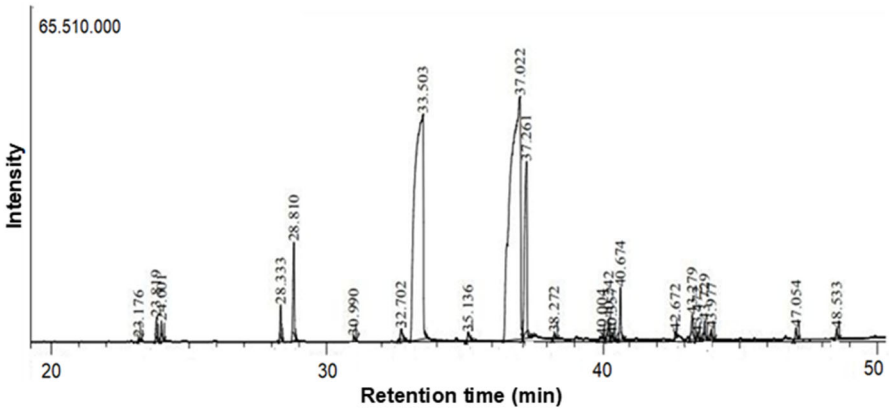


**Fig 5.** GC-MS Chromatogram of biodiesel from CPO using CaO-$SiO_2$ (5%) catalyst

**Table 8.** FAME content in biodiesel from CPO using CaO-$SiO_2$ (5%) catalyst

| Methyl ester (Formula) | Retention time (min) | MW | Peak area (%) |
|---|---|---|---|
| Methyl laurate ($C_{13}H_{26}O_2$) | 24.001 | 214 | 0.490 |
| Methyl myristate ($C_{15}H_{30}O_2$) | 28.819 | 242 | 2.690 |
| Methyl pentadecanoate ($C_{16}H_{32}O_2$) | 30.990 | 256 | 0.130 |
| Methyl palmitoleate ($C_{17}H_{32}O_2$) | 32.702 | 268 | 0.410 |
| Methyl palmitate ($C_{17}H_{34}O_2$) | 33.503 | 270 | 35.450 |
| Methyl margarate ($C_{18}H_{36}O_2$) | 35.136 | 284 | 0.320 |
| Methyl oleate ($C_{19}H_{36}O_2$) | 37.022 | 296 | 45.530 |
| Methyl stearate ($C_{19}H_{38}O_2$) | 37.261 | 298 | 7.950 |
| Methyl linoleate ($C_{19}H_{34}O_2$) | 38.272 | 294 | 0.140 |
| Methyl eicosatrienoate ($C_{21}H_{36}O_2$) | 40.004 | 320 | 0.170 |
| Methyl 11-eicosenoate ($C_{21}H_{40}O_2$) | 40.242 | 324 | 0.590 |
| Methyl ketostearate ($C_{19}H_{36}O_3$) | 40.357 | 312 | 0.160 |
| Methyl arachate ($C_{21}H_{42}O_2$) | 40.674 | 326 | 1.300 |
| Methyl 9,10-dihydroxystearate ($C_{19}H_{38}O_4$) | 43.472 | 330 | 1.030 |
| Methyl dichlorostearate ($C_{19}H_{36}Cl_2O_2$) | 43.729 | 366 | 0.530 |
| Methyl behenate ($C_{23}H_{46}O_2$) | 43.977 | 354 | 0.270 |
| Methyl lignocerate ($C_{25}H_{50}O_2$) | 47.054 | 382 | 0.280 |

**Table 9.** The properties of biodiesel from CPO using CaO-$SiO_2$ (5%)

| Characterization | Units | ASTM D6751 | This biodiesel |
|---|---|---|---|
| Methyl ester content | % | 96.5 (EN 14214) | 97.44 |
| Water content | %(v/v) | Max. 0.05 | 0.03 |
| Density 40 °C | kg $m^{-3}$ | 860–900 | 886 |
| Viskosity 40 °C | $mm^2$ $s^{-1}$ | 3.5–6.0 | 4.97 |
| Carbon residue | % | Max. 0.05 | 0.00 |
| Acid content | mg-KOH $g^{-1}$ | Max. 0.5 | 1.70 |

from palm oil shows a good balance between oxidation stability and flow properties at low temperatures, making it an efficient and sustainable alternative fuel for diesel engines [37].

The results of this characterization were then compared to the biodiesel quality standards outlined in ASTM D6751 and EN 14214 and the results are shown in Table 9. The properties of biodiesel from CPO were

assessed under operating conditions of a 3 wt.% catalyst concentration and a reaction time of 60 min, using the EN 14214 standard method for biofuels, as summarized in Table 9. Under these conditions, the biodiesel achieved its highest yield of 96.29% with a methyl ester content of 97.44%, significantly higher than the methyl ester content of 88.14% obtained when using a CaO catalyst. The resulting viscosity, density, carbon residue and acid content were 4.97 $mm^2 s^{-1}$, 886 $kg m^{-3}$, 0%, 1.7 mg-KOH $g^{-1}$, respectively, all of which fall within the acceptable ranges of the ASTM D6751 and EN 14214 standards, except for acid number. This confirms that biodiesel produced from CPO with CaO-$SiO_2$ solid base catalyst can be classified as a suitable biodiesel fuel.

## ■ CONCLUSION

The modification of CaO derived from blood cockle shells with $SiO_2$ from coconut husk ash has proven to be an effective heterogeneous catalyst for biodiesel production, particularly with oils containing high FFA content, such as CPO. The impregnation of $SiO_2$ onto CaO enhances catalytic activity, leading to a significant increase in biodiesel yield. Optimal biodiesel production conditions were achieved using a CaO-$SiO_2$ catalyst with 5% $SiO_2$ composition, 2 wt.% catalyst loading, a reaction time of 90 min, a temperature of 60 °C, resulting in a biodiesel yield of 96.29% with a purity of 97.44%.

## ■ ACKNOWLEDGMENTS

The authors gratefully acknowledge the financial support of this project from University of Riau through the DIPA LPPM Riau University under *Bidang Ilmu* Grant (8258/UN19.5.1.3/AL.04/2023).

## ■ CONFLICT OF INTEREST

There are no conflict of interest in this article.

## ■ AUTHOR CONTRIBUTIONS

Nurhayati contributed to the study conception and design. Data collection and analysis were performed by Nurhayati, Muhdarina and Amilia Linggawati. Nurhayati and Siti Saidah Siregar wrote and revised the manuscript. All authors approved the final version of this manuscript.

## ■ REFERENCES

[1] Awogbemi, O., Kallon, D.V.V., and Aigbodion, V.S., 2021, Trends in the development and utilization of agricultural wastes as heterogeneous catalyst for biodiesel production, *J. Energy Inst.*, 98, 244–258.

[2] Nurhayati, N., Anita, S., Amri, T.A., and Linggawati, A., 2017, Esterification of crude palm oil using $H_2SO_4$ and transesterification using CaO catalyst derived from *Anadara granosa*, *Indones. J. Chem.*, 17 (2), 309–315.

[3] Nurhayati, N., Anita, S., Amri, T.A., and Muhdarina, M., 2018, The effects of catalyst weight and mole ratio of oil-methanol on crude palm oil (CPO) esterification using $H_2SO_4$ (3M)/clay catalyst, *J. Phys.: Conf. Ser.*, 1093 (1), 012006.

[4] Nurhayati, N., Amri, T.A., Annisa, N.F., and Syafitri, F., 2020, The synthesis of biodiesel from crude palm oil (CPO) using CaO heterogeneous catalyst impregnated $H_2SO_4$, variation of stirring speed and mole ratio of oil to methanol, *J. Phys.: Conf. Ser.*, 1655 (1), 012106.

[5] Elias, S., Rabiu, A.M., Okeleye, B.I., Okudoh, V., and Oyekola, O., 2020, Bifunctional heterogeneous catalyst for biodiesel production from waste vegetable oil, *Appl. Sci.*, 10 (9), 3153.

[6] Basumatary, S.F., Brahma, S., Hoque, M., Das, B.K., Selvaraj, M., Brahma, S., and Basumatary, S., 2023, Advances in CaO-based catalysts for sustainable biodiesel synthesis, *Green Energy Resour.*, 1 (3), 100032.

[7] Nurhayati, N., Muhdarina, M., Linggawati, A., Anita, S. and Amri, T.A., 2016, Preparation and characterization of calcium oxide heterogeneous catalyst derived from *Anadara granosa* shell for biodiesel synthesis, *KnE Eng.*, 2016, 494.

[8] Li, H., Niu, S., Lu, C., and Li, J., 2016, Calcium oxide functionalized with strontium as heterogeneous transesterification catalyst for biodiesel production, *Fuel*, 176, 63–71.

[9] Mansir, N., Teo, S.H., Rabiu, I., and Taufiq-Yap, Y.H., 2018, Effective biodiesel synthesis from waste

cooking oil and biomass residue solid green catalyst, *Chem. Eng. J.*, 347, 137–144.

[10] Pandiangan, K.D., Simanjuntak, W., Ilim, I., Satria, H., and Jamarun, N., 2019, Catalytic performance of $CaO/SiO_2$ prepared from local limestone industry and rice husk silica, *J. Pure Appl. Chem. Res.*, 8 (2), 170–178.

[11] Alias, N.S.M., Veny, H., Hamzah, F., and Aziz, N., 2019, Effect of free fatty acid pretreatment to yield, composition and activation energy in chemical synthesis of fatty acid methyl ester, *Indones. J. Chem.*, 19 (3), 592–598.

[12] Kesserwan, F., Ahmad, M.N., Khalil, M., and El-Rassy, H., 2020, Hybrid $CaO/Al_2O_3$ aerogel as heterogeneous catalyst for biodiesel production, *Chem. Eng. J.*, 385, 123834.

[13] Sisca, V., Deska, A., Syukri, S., Zilfa, Z., and Jamarun, N., 2021, Synthesis and characterization of CaO limestone from Lintau Buo supported by $TiO_2$ as a heterogeneous catalyst in the production of biodiesel, *Indones. J. Chem.*, 21 (4), 979–989.

[14] Ngaosuwan, K., Chaiyariyakul, W., Inthong, O., Kiatkittipong, W., Wongsawaeng, D., and Assabumrungrat, S., 2021, $La_2O_3/CaO$ catalyst derived from eggshells: Effects of preparation method and La content on textural properties and catalytic activity for transesterification, *Catal. Commun.*, 149, 106247.

[15] Nurhayati, N., Saputra, L., Awaluddin, A., and Kurniawan, E., 2021, Converting waste cooking oil to biodiesel catalyzed by NaOH-impregnated CaO derived from cockle shell (*Anadara granosa*), *Kinet. Catal.*, 62 (6), 860–865.

[16] Lani, N.S., Ngadi, N., and Inuwa, I.M., 2010, New route for the synthesis of silica supported calcium oxide catalyst in biodiesel production, *Renewable Energy*, 156, 1266–1277.

[17] Lani, N.S., Ngadi, N., Yahya, N.Y., and Rahman, R.A., 2016, Synthesis, characterization and performance of silica impregnated calcium oxide as heterogeneous catalyst in biodiesel production, *J. Cleaner Prod.*, 146, 116–124.

[18] Anuar, M.F., Fena, Y.W., Mohd Zaid, M.H., Matori, K.A., and Khaidir, R.E.M., 2018, Synthesis and structural properties of coconut husk as potential silica source, *Results Phys.*, 11, 1–4.

[19] Anuar, M.F., Fen, Y.W., Mohd Zaid, M.H., Matori, K.A., and Khaidir, R.E., 2020, The physical and optical studies of crystalline silica derived from green synthesis of coconut husk ash, *Appl. Sci.*, 10 (6), 2128.

[20] Chumuang, N., and Punsuvon, V., 2017, Response surface methodology for biodiesel production using calcium methoxide catalyst assisted with tetrahydrofuran as cosolvent, *J. Chem.*, 2017 (1), 4190818.

[21] Tamoradi, T., Kiasat, A.R., Veisi, H., Nobakht, V., and Karmakar, B., 2022, RSM process optimization of biodiesel production from rapeseed oil and waste corn oil in the presence of green and novel catalyst, *Sci. Rep.*, 12 (1), 19652.

[22] Fiquet, G., Richet, P., and Montagnac, G., 1999, High-temperature thermal expansion of lime, periclase, corundum and spinel, *Phys. Chem. Miner.*, 27 (2), 103–111.

[23] Sahu, G., Saha, S., Datta, T., Chavan, P., and Naik, S., 2017, Methanolysis of *Jatropha curcas* oil using $K_2CO_3/CaO$ as a solid base catalyst, *Turk. J. Chem.*, 41 (6), 845–867.

[24] Xin, B., Le Febvrier, A., Shu, R., Elsukova, A., Venkataramani, V., Shi, Y., Ramanath, G., Paul, B., and Eklund, P., 2021, Engineering faceted nanoporosity by reactions in thin-film oxide multilayers in crystallographically layered calcium cobaltate for thermoelectrics, *ACS. Appl. Nano Mater.*, 4 (9), 9904–9911.

[25] Hadiyanto, H., Lestari, S.P., Abdullah, A., Widayat, W., and Sutanto, H., 2016, The development of fly ash-supported CaO derived from mollusk shell of *Anadara granosa* and *Paphia undulata* as heterogeneous CaO catalyst in biodiesel synthesis, *Int. J. Energy Environ. Eng.*, 7 (3), 297–305.

[26] Moosa, A.A., and Saddam, B.F., 2017, Synthesis and characterization of nanosilica from rice husk with

applications to polymer composites, *Am. J. Mater. Sci.*, 7 (6), 223–231.

[27] Langford, J.I., and Wilson, A.J.C., 1978, Scherrer after sixty years: A survey and some new results in the determination of crystallite size, *J. Appl. Crystallogr.*, 11 (2), 102–113.

[28] Hou, Y., Zhang, G.H., Chou, K.C., and Fan, D., 2020, Effects of $CaO/SiO_2$ ratio and heat treatment parameters on the crystallization behavior, microstructure and properties of $SiO_2$-CaO-$Al_2O_3$-$Na_2O$ glass ceramics, *J. Non-Cryst. Solids*, 538, 120023.

[29] Wu, J., Liao, H., Ma, Z., Song, H., and Cheng, F., 2023, Effect of different initial $CaO/SiO_2$ molar ratios and curing times on the preparation and formation mechanism of calcium silicate hydrate, *Materials*, 16 (2), 717.

[30] Fatimah, I., Fadillah, G., Sagadevan, S., Oh, W.C., and Ameta, K.L., 2023, Mesoporous silica-based catalysts for biodiesel production: A review, *ChemEngineering*, 7 (3), 56.

[31] Jamil, N.H., Abdullah, S.A., and Modh Zarib, N.S., 2019, Extraction of silica from rice husk via acid leaching treatment, *Eur. Proc. Soc. Behav. Sci.,* 62, 175–183.

[32] Davis, R.J., 2000, Relationships between basicity and reactivity of zeolite catalysts, *Res. Chem. Intermed.*, 26, 21–27.

[33] Verdoliva, V., Saviano, M., and De Luca, S., 2019, Zeolites as acid/basic solid catalysts: Recent synthetic developments, *Catalysts*, 9 (3), 248.

[34] Ngige, G.A., Ovuoraye, P.E., Igwegbe, C.A., Fetahi, E., Okeke, J.A., Yakubu, A.D., and Onyechi, P.C., 2023, RSM optimization and yield prediction for biodiesel produced from alkali-catalytic transesterification of pawpaw seed extract: Thermodynamics, kinetics, and multiple linear regression analysis, *Digital Chem. Eng.*, 6, 100066.

[35] Maulidiyah, M., Watoni, A.H., Maliana, N., Irwan, I., Salim, L.O.A., Arham, Z., and Nurdin, M., 2022, Biodiesel production from crude palm oil using sulfuric acid and $K_2O$ catalysts through a two-stage reaction, *Biointerface Res. Appl. Chem.*, 12 (3), 3150–3160.

[36] Lani, N.S., Ngadi, N., and Taib, M.R., 2017, Parametric study on the transesterification reaction by using CaO/silica catalyst, *Chem. Eng. Trans.*, 56, 601–606.

[37] Knothe, G., and Razon, L.F., 2017, Biodiesel fuels, *Prog. Energy Combust. Sci.,* 58, 36–59.